CISK AS A BASIS FOR CONVECTIVE PARAMETERISATION IN BAROCLINIC FLOWS - APPLICATION TO FRONTAL DEVELOPMENT

A.J. Thorpe
Department of Meteorology
University of Reading
Reading, U.K.

Abstract:

Convection often exhibits mesoscale organization in the atmosphere. In recent years a dynamical description of the mesoscale has been formulated and it is now appropriate to consider the representation of fundamentally mesoscale phenomena in large-scale models. Both theory and observations of frontal systems indicate the crucial role of the mesoscale, $L \sim V/f$, in mid-latitude cyclones. Much precipitation in mid-latitudes is associated with such systems whilst the large-scale models cannot resolve their detailed structure. In this paper, therefore, the recently developed theories of convection forced by frontogenesis and by mesoscale instabilities are reviewed. Several ideas for parameterisation in large-scale models are presented but detailed schemes await further theoretical work.

1. INTRODUCTION

The existence and description of the mesoscale has become an increasingly important problem in the theoretical study of the basic dynamics of the atmosphere and for parameterisation in large-scale models. The definition of the term mesoscale is an illustrative example of the difficulties of this subject. Observations of atmospheric phenomena have led to grouping into mesoscale such diverse systems as severe local storms, mountain waves, fronts, and sea breezes. Indicative of the fuzzy nature of such a definition of mesoscale is the need to subdivide into further classes meso α, β, and γ (Orlanski, 1975). This discussion would be of purely semantic interest if it were not for the emergence of a dynamical definition of the mesoscale which allows consideration of a hierarchy of scale interactions - large-scale $\rightarrow$ mesoscale $\rightarrow$ cloud scale - and attendant parameterisation problems. In some, perhaps many, cases parameterisation has been attempted of the cloud scale into large-scale models without consideration of the mesoscale. Whilst this may be successful in some cases, for example, tropical convection, it may be less well-posed for mid-latitude systems.

The emergence of high resolution mesoscale numerical models (horizontal grid-length $\sim$ 20 km) may provide a bridge to enable specifically mesoscale parameterisation schemes to emerge. It seems worth-while to restate the more-or-less obvious concept that to parameterise a scale of motion it first has to be understood and modelled

explicitly. An example is that of tropical squall lines which have been modelled using simple analytical and cloud-scale numerical models (Moncrieff and Miller, 1976) and so parameterisation schemes for momentum and heat fluxes can be devised for inclusion in larger-scale models (see article by Moncrieff and Miller in this volume). To take the example to be described in this paper, it would be difficult to imagine representing moist processes at fronts in large-scale models without understanding the mesoscale.

Implicit in the hierarchy of scales is that there exist identifiable peaks in the energy spectrum. The existence of a mesoscale peak has long been the subject of some controversy and it may be that routine data have insufficient resolution to adequately define mesoscale structures. At any rate a cursory glance at weather charts of mid-latitudes shows a dominant mesoscale organisation to be fronts and their association precipitation bands. The theory of frontogenesis has been an important development in dynamical meteorology in the last ten years and has helped to provide a dynamical definition of the mesoscale. As will be discussed later, the quasi-geostrophic equations only allow the formation of a sharp front in an infinite time and are therefore inadequate in describing realistic frontogenesis. Consequently the semi-geostrophic equations were developed in which the advection by both the geostrophic *and* ageostrophic components of the flow are important. These equations capture the collapse of frontal scale in a finite time. Inherent in this description is the importance of the earth's rotation and ageostrophic advection and this leads to the motion being characterised by Rossby number $Ro \sim 1$. Consequently it is consistent that the typical length scale $L \sim V/f$ or $V_z H/f$. Typical values give $L \sim 100$ km which defines a mesoscale. In the frontal case therefore there is a relatively clear distinction between horizontal scales of large scale ($Ro \ll 1$, $L = NH/f \sim 1000$ km), mesoscale ($Ro \sim 1$, $L = V_z H/f \sim 100$ km), and cloud scale ($Ro \gg 1$, $L = H \sim 10$ km).

A distinction is now apparent between fronts and, say, deep convection. The latter is frequently referred to as mesoscale although the dynamics of deep convection can be adequately described by neglecting the effects of the earth's rotation; see, for example, Thorpe, Miller and Moncrieff (1982). The horizontal scale of anvil cloud can be of order several hundred kilometres but this represents advection of a more-or-less passive tracer - the scale of active dynamics in, say, the updraught is of order 10 km. Subsidence around the cloud can be of larger scale than that of the cloud but its dynamical structure may not require the effects of rotation to be included.

Frontogenesis is only one example of a phenomenon which involves dynamics on the mesoscale. Inertio-gravity waves, sea-breeze circulations and symmetric instability are other example of mesoscale phenomena by this dynamical definition. A more

detailed description of the concept of the mesoscale can be found in Emanuel (1983).

Alongside these improvements in our understanding of the mesoscale, in particular with reference to frontal systems, there have been observational programmes to collect mesoscale data, and also development of numerical models. As these data, from both sources, are assimilated it is timely to consider what implications this progress has for large-scale models and numerical weather prediction in general. However, the observational data sets are, as yet, incomplete and as new field experiments are planned it is important to determine not only detailed dynamical hypotheses to be tested but also the uses of such data sets in initialization of mesoscale models and in developing parameterisation schemes for large-scale models.

This contribution to the workshop will attempt to review mesoscale aspects of frontal convection and suggest various possibilities for parameterisation schemes. Amongst these will be a scheme using the mathematical form of CISK although, as stated by Ooyama (1982), it may be inappropriate to label such a theory in this way. It has become, perhaps unfortunately, suggestive of a particular representation of diabatic heating rather than of the original idea. The review aspects of this paper draw heavily on published and unpublished work by Professors B.J. Hoskins and K.A. Emanuel, amongst others, and on current research of the author. Many speculative ideas will be presented which may prove to be incorrect finally but which are intended as points for discussion and further development.

The paper is divided into three main sections followed by a discussion. In section 2 the role of frontogenesis in forcing convective organization is described and the point is made that as latent heat is released in the forced ageostrophic circulations the baroclinic flow can become dynamically unstable to small disturbances. In this way symmetric instability may occur and the structure of these mesoscale instabilities is reviewed in section 3. The instability organizes the convection on the mesoscale and in a sense determines the structure of sloping convection in baroclinic flows. Prospects for parameterization of convection at fronts are considered in section 4 and various ideas for future work are presented.

2. CONVECTION FORCED BY FRONTOGENESIS

2.1 Summary of two-dimensional frontogenesis

Although atmospheric fronts have three-dimensional features it is adequate for the present purposes to confine the discussion to two-dimensional dynamics.

The diabatic, Boussinesq, hydrostatic equations may be written using conventional notation as:

$$\frac{Du}{Dt} - fv + \frac{\partial \phi}{\partial x} = \underline{\nabla} \cdot (\overline{k\nabla}\, u) \tag{1}$$

$$\frac{Dv}{Dt} + fu + \frac{\partial \phi}{\partial y} = \underline{\nabla} \cdot (\overline{k\nabla}\, v) \tag{2}$$

$$\frac{\partial \phi}{\partial z} = g \frac{\theta}{\theta_0} \tag{3}$$

$$\underline{\nabla} \cdot \underline{v} = 0 \tag{4}$$

$$\frac{D\theta}{Dt} = B + \underline{\nabla} \cdot (\overline{k\nabla}\, \theta) \tag{5}$$

where $\overline{k\nabla} = \left(k_x \frac{\partial}{\partial x}, k_y \frac{\partial}{\partial y}, k_z \frac{\partial}{\partial z} \right)$ and a Prandtl number of unity has been assumed. The function B represents diabatic heat sources and sinks.

Two-dimensionality is assumed in the sense that, if y is an axis along the front, then all y derivatives are zero except for $\partial\phi/\partial y$, $\partial\theta/\partial y$ and $\partial v/\partial y$. If typical velocities U and V and length scale L are used to scale terms in equation (1), it is apparent that

$$\frac{Du}{Dt} \ll fv \quad \text{if} \quad \left(\frac{V}{fL}\right)\left(\frac{U}{V}\right) \ll 1 \tag{6}$$

$$k\nabla^2 u \ll fv \text{ if } \left(\frac{k}{fL^2}\right)\left(\frac{U}{V}\right) \ll 1 \quad . \tag{7}$$

Values typical for a front are U = 2 m s^{-1}, V = 20 m s^{-1}, L = 100 km, and $k \lesssim 10^5$ m^2 s^{-1}. Thus the inequalities in these equations are easily satisfied. Therefore equation (1) shows that to a good approximation v is given by the geostrophic value for all time.

It is convenient to make a decomposition into the geostrophic and ageostrophic flow:

$$u = u_g(x,z) + u_a(x,z,t) \quad , \quad u_g = -\frac{1}{f}\frac{\partial \phi}{\partial y} \quad .$$

Making the above approximations allows the equations to be written in the form:

$$v = \frac{1}{f}\frac{\partial \phi}{\partial x} \tag{8}$$

$$\frac{Dv}{Dt} + fu_a = \underline{\nabla} \cdot (\overline{k\nabla}\, v) \tag{9}$$

$$\frac{D\theta}{Dt} = B + \underline{\nabla} \cdot (\overline{k\nabla}\, \theta) \tag{10}$$

$$\frac{\partial u_g}{\partial x} + \frac{\partial v}{\partial y} = 0 \tag{11}$$

$$\frac{\partial u_a}{\partial x} + \frac{\partial w_a}{\partial z} = 0 \tag{12}$$

The thermal wind balances and Brunt-Väisälä frequency are defined as follows:

$$\left.\begin{aligned} \frac{\partial u_g}{\partial z} &= -\frac{g}{f\theta_0}\frac{\partial \theta}{\partial y} \\ \frac{\partial v}{\partial z} &= \frac{g}{f\theta_0}\frac{\partial \theta}{\partial x} \\ N^2 &= \frac{g}{\theta_0}\frac{\partial \theta}{\partial z} \quad . \end{aligned}\right\} \tag{13}$$

The equation for the cross-frontal circulation can be obtained from these equations by constructing $f\frac{\partial}{\partial z}$ (9) $-\frac{g}{\theta_0}\frac{\partial}{\partial x}$ (10) and using the thermal wind equations:

$$N^2 \psi_{xx} - 2S^2 \psi_{xz} + F^2 \psi_{zz} = -2Q - \frac{g}{\theta_0} B_x + DF \tag{14}$$

where the basic flow frequencies are defined as:

$$S^2 = f\frac{\partial v}{\partial z} \quad , \quad F^2 = f\left(f + \frac{\partial v}{\partial x}\right)$$

and the diffusion term DF is given by the equation:

$$DF = f\frac{\partial}{\partial x}\left[\frac{\partial k_x}{\partial z}\frac{\partial v}{\partial x} - \frac{\partial k_x}{\partial x}\frac{\partial v}{\partial z}\right] + f\frac{\partial}{\partial z}\left[\frac{\partial k_z}{\partial z}\frac{\partial v}{\partial z} - \frac{\partial k_z}{\partial x}\frac{N^2}{f}\right] \quad .$$

It should be noted that DF is zero if there are constant, but non-zero, diffusion coefficients, and this will be assumed in what follows.

The quantity Q is the x-component of a vector which specifies the synoptic-scale forcing of the ageostrophic circulation about fronts:

$$Q = f\left(\frac{\partial u_g}{\partial z}\frac{\partial v}{\partial x} - \frac{\partial u_g}{\partial x}\frac{\partial v}{\partial z}\right) \quad .$$

The first term in the bracket represents the forcing due to deformation whilst the second that due to shear.

The circulation equation (14) is an elliptic equation if the potential vorticity $q = F^2N^2 - S^4 > 0$ everywhere in the fluid. On the other hand, if $q < 0$ then the equation is hyperbolic and symmetric instability is possible *(see section 3)*.

The potential vorticity equation can be shown to be given by:

$$\frac{Dq}{Dt} = \frac{fg}{\theta_0}\left[\frac{\partial v}{\partial x}\frac{\partial B}{\partial z} - \frac{\partial v}{\partial z}\frac{\partial B}{\partial x}\right] + DQ \tag{15}$$

where DQ is the diffusion term.

In summary, the equations (9) for v and (10) for θ (or alternatively (15) for q) determine the evolution of the flow whilst the circulation equation is diagnostic giving the ageostrophic flow at any time. These equations are referred to as semi-geostrophic as the substantial derivative involves advection by the total flow and not just the geostrophic component as in the quasi-geostrophic approximation. These equations have been the subject of analytical (Hoskins and Bretherton, 1972) and numerical solution (e.g. Hoskins and Heckley, 1981) to show the formation of sharp

fronts in a finite time.

The circulation equation can be written in a compact way using the geostrophic momentum coordinates X and Z

$$X = x + v/f \quad , \quad Z = z$$

to give:

$$\frac{(q\,\psi_X)_X}{f^4} + \psi_{ZZ} = -\frac{2Q}{F^2} - \frac{g}{\theta_0 f^2} B_X \quad . \tag{16}$$

This equation derived by Eliassen (1962) shows, among other things, that the circulation about a region of positive Q, in the absence of diabatic forcing, is in the form of a thermally direct flow (warm air rising, colder air sinking) whose axis lies along constant X-surfaces. The slope of the X-surface is given by $dx/dz = -v_z/(f + v_x) = -S^2/F^2$ and this expression leads to the dynamical motion of the mesoscale ($L \sim v_z H/f$).

A final equation of particular interest is that for the rate of change of frontogenesis function $\frac{1}{2}\theta_x^2$ describing the tendency of the temperature gradient to intensify:

$$\frac{D}{Dt}\left(\tfrac{1}{2}\theta_x^2\right) = \theta_x \left[\frac{f\theta_0}{g}\left(Q - \frac{\partial v}{\partial z}\frac{\partial u_a}{\partial x} - \frac{N^2}{f}\frac{\partial w_a}{\partial x}\right) + \frac{\partial B}{\partial x} + \frac{\partial}{\partial x}\left(\underline{\nabla} \cdot (k\overline{\nabla\theta})\right)\right] . \tag{17}$$

It is clear from equation (17) that the rate of change of frontogenesis following the flow has contributions from geostrophic forcing, the ageostrophic flow, diabatic heating and diffusion.

In this paper the role of the diabatic term in these equations will be discussed to illuminate the role of convection at fronts. This section will be concerned with the case $q > 0$ and $Q \neq 0$ which contains the possibility of convection forced by frontogenesis. In contrast, section 3 will consider the case $q < 0$ and $Q = 0$ which describes convective mesoscale instabilities ('rainbands') in a baroclinic region remote from frontogenetic forcing. The most interesting, and least understood, case is of a region in which q can have local minima but which has $Q \neq 0$ and is therefore frontogenetic. Possible parameterisation schemes in this case are discussed in section 4.

2.2 Diabatic heating in an unforced baroclinic flow

Before describing convection forced by frontogenesis, it is instructive to consider the response of a baroclinic flow to an arbitrary local diabatic source when there is no frontogenetic forcing. In this case $Q = 0$ and equation (16) becomes:

$$\frac{(q\,\psi_X)_X}{f^4} + \psi_{ZZ} = -\frac{g}{\theta_0 f^2} B_X \quad . \tag{18}$$

The solution to this equation was first described by Eliassen (1952) and later by Charney (1973), and has since been used by many authors (for more details see Gill (1982) pp 362-366). In Figure 1 the response to a point source heating function is described.

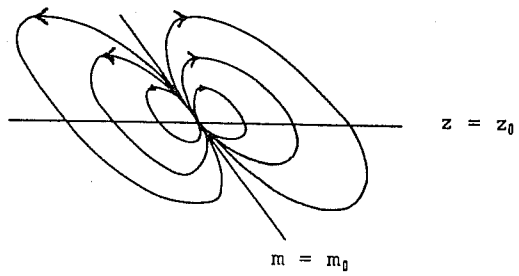

Figure 1. Response to point source heating

The quantity $m = X f = v + fx$ is the absolute momentum.

The response is of vertical motion along a constant m (or X) surface through the source with compensating descent given by potential flow in the scaled coordinates (X,Z). In the atmosphere m surfaces are not necessarily straight lines and the line segment in the figure is a local tangent to the m surface at the source. Therefore in the case of diabatic forcing, as well as Q-forcing, the motion is orientated along X surfaces which, it should be noted, are not constant θ-surfaces. This point is of some importance to the later discussion and can be clarified by considering the simplest case of a uniform baroclinic zone given by the formulae:

$$\begin{aligned} \theta &= \frac{\theta_0}{g}\,(S^2 x + N^2 z) \\ v &= v_x x + v_z z \\ m &= \frac{1}{f}\,(F^2 x + S^2 z) \end{aligned} \qquad (19)$$

where all gradients are constants.

Thus the slopes of the θ, v, and m surfaces are given as follows:

$$\left(\frac{dx}{dz}\right)_\theta = -\frac{N^2}{S^2}\ , \quad \left(\frac{dx}{dz}\right)_v = \frac{v_z}{v_x}\ , \quad \left(\frac{dx}{dz}\right)_m = -\frac{S^2}{F^2}\ ,$$

where it can be shown that

$$\left(\frac{dx}{dz}\right)_\theta \lesseqgtr \left(\frac{dx}{dz}\right)_m \quad \text{if } q \gtreqless 0\ .$$

Of course the slow, steady response shown in figure 1 is only applicable in the case $q > 0$.

In summary, it is apparent immediately that in a baroclinic flow heating due to condensation produces a circulation oriented along absolute momentum surfaces and this is suggestive of the notion of sloping convection. In a baroclinic zone such

as a front with large velocity gradients $|(dx/dz)_m|$ can be rather large ($\gtrsim 50$) suggesting a shallow slope to the latent heat release.

2.3 Diabatic heating in a forced baroclinic flow

The circulation equation (16) shows that the motion produced either by geostrophic forcing (Q) or by diabatic forcing (B_X) tends to align along absolute momentum surfaces. This suggests that in a frontogenetic situation latent heating will tend to enhance that upward motion in the ageostrophic circulation present in the dry case. However it would appear that the descending return flow induced by the heating, shown in figure 1, could disrupt the thermally direct circulation produced by positive geostrophic forcing. As will be shown in this section, the precise dependence of the diabatic term on the motion itself leads to two rather distinct regimes.

There are two relatively simple ways to represent the dependence of latent heating on the motion which highlight the different regimes. The first imagines the diabatic term to be proportional to the vertical velocity and imagines parcel ascent and descent along a constant θ_w trajectory:

$$\frac{D\theta}{Dt} = B = \gamma w \qquad \text{or} \qquad \frac{D\theta_w}{Dt} = 0 \tag{20}$$

where $\gamma \sim \frac{L}{c_p} \frac{\partial}{\partial z} r_{sat}$, and r is the specific humidity. This is equivalent to fluid parcels remaining saturated on vertical motion. Substituting this form for B into the circulation equation (14) gives

$$N_w^2 \psi_{xx} - 2S^2 \psi_{xz} + F^2 \psi_{zz} = -2Q \tag{21}$$

where N_w is the Brunt-Väisälä frequency based on the lapse rate of wet-bulb potential temperature. This shows that the circulation with diabatic forcing is equivalent to that in a region of reduced static stability and that the presence of the heat source does not change the form of the flow. The equation is elliptic as long as $q > F^2(N^2 - N_w^2)$ or $q_w = F^2 N_w^2 - S^4 > 0$ or $\gamma < q/F^2$.

A similar result can be derived if the heating only occurs on ascent, i.e.

$$B = \frac{\gamma}{2}(w + |w|)$$

$$(1 + \mathrm{sgn}(w)) \frac{N_w^2}{2} \psi_{xx} - 2S^2 \psi_{xz} + F^2 \psi_{zz} = -2Q \quad , \tag{22}$$

where $\mathrm{sgn}(w) = 1$ if $w > 0$

$= -1$ if $w < 0$.

Therefore a parameterisation such as that in equation (20) simply increases the circulation existing without the diabatic forcing. Solutions to a form of equation (22) can be found in Sawyer (1956) and later in this article.

An alternative parameterisation of latent heat release is to imagine that it is dependent on moisture convergence in the boundary layer. If this occurs in an atmosphere that is conditionally unstable then convection will be triggered. Such a region of deep convection would produce heating in a vertical column above the boundary layer convergence and is likely to contain many convective elements of scale ($L \sim H$) considerably smaller than that of the region itself ($L \sim v/f$). In contrast to the previous representation of the diabatic term which described latent heat release following a parcel, this form parameterises a region of statistically steady convection. As such the diabatic term is due to adiabatic warming caused by subsidence balancing the mass flux in individual element updraughts. This formulation relies on a scale separation between the convective elements and the mesoscale band. It is convenient, if not entirely accurate to the original concept, to label this parameterisation scheme as being of CISK type. The mathematical form of B in this case is as follows:

$$B = \frac{\theta_0}{g} N^2 b(z) \left(w_{z_0} + |w_{z_0}|\right) \quad , \tag{23}$$

where $w_{z_0} = w(z = z_0)$ and z_0 is typically the height of the top of the boundary layer. The presence of N^2 in equation (23) is indicative of the role of subsidence warming in this scheme. The function $b(z)$ is known as the structure function and determines the vertical distribution of diabatic forcing. As this is not determined by the flow itself it remains the least satisfactory aspect of CISK-type schemes.

The latter scheme (CISK) has been used in Thorpe and Nash (1983) and Thorpe (1983) and solutions to the circulation equation were obtained for a frontal structure with a jet. In figure 2 the velocity and potential temperature structure is shown along with the Q forcing resulting from a constant deformation field. Figures 3 and 4 show the ageostrophic circulation about the front with B = 0, B from equation (22), and CISK form of B from equation (23). It can be seen that the CISK form (figure 4) produces a disruption of the circulation by introducing descent in the warm air. This is a consequence of the phase difference between the heating (constant on x-surfaces) and the inherent motion (constant along m-surfaces). The circulation with diabatic heating of this type represents the response not to sloping convection but to more vigorous upright convective elements. This phase difference is of some importance in the discussion of the symmetric CISK instability to be described in section 3.2, and is responsible in that case for there being a wavelength of maximum growth. These instabilities are not present in the solutions just described.

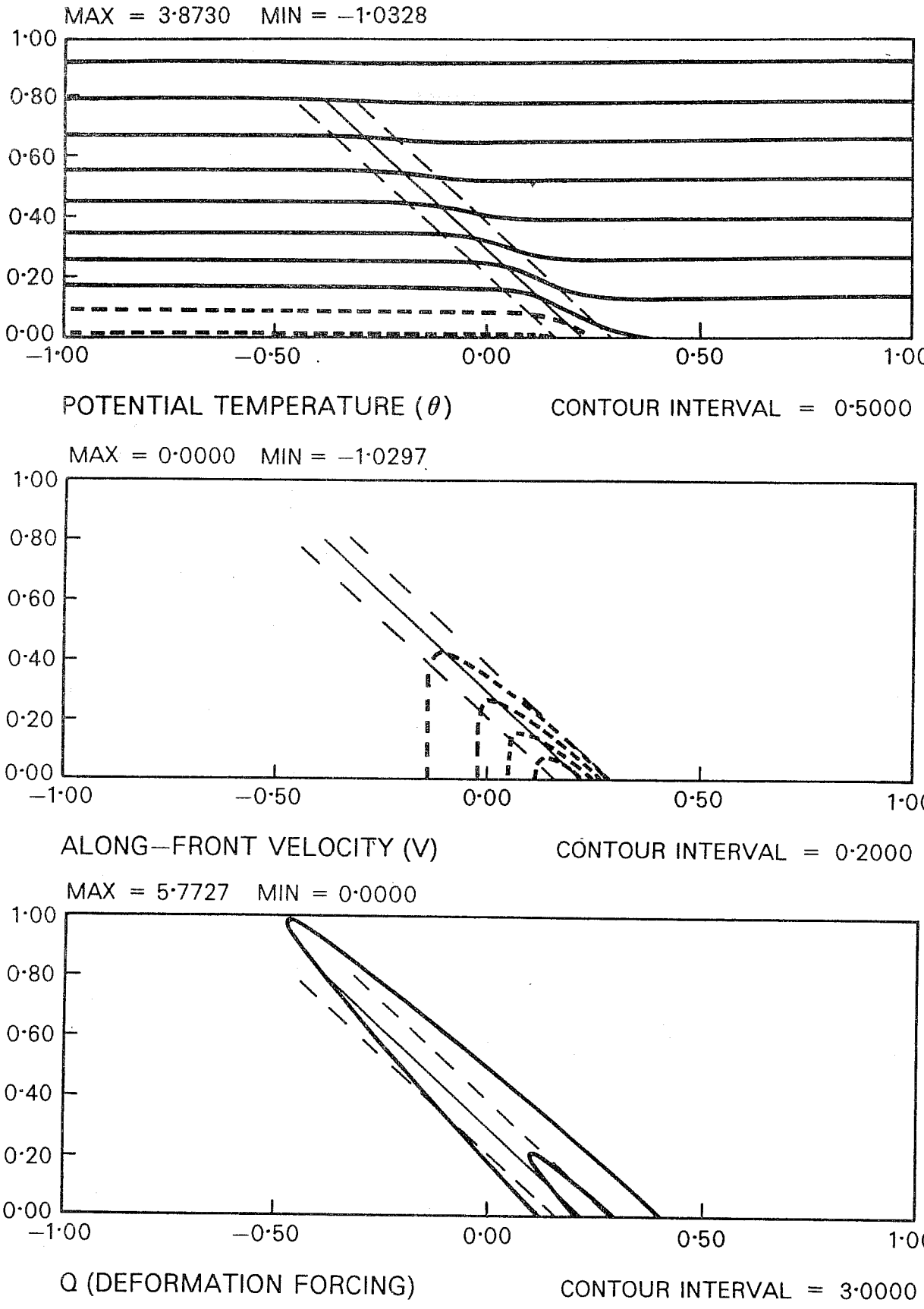

Figure 2. Basic geostrophic structure and forcing for a cold front situation taken from Thorpe and Nash (1984). Thin solid and dashed lines indicate the location of the frontal transition zone. The horizontal dimension is scaled with the Rossby radius of deformation based on the height of the domain.

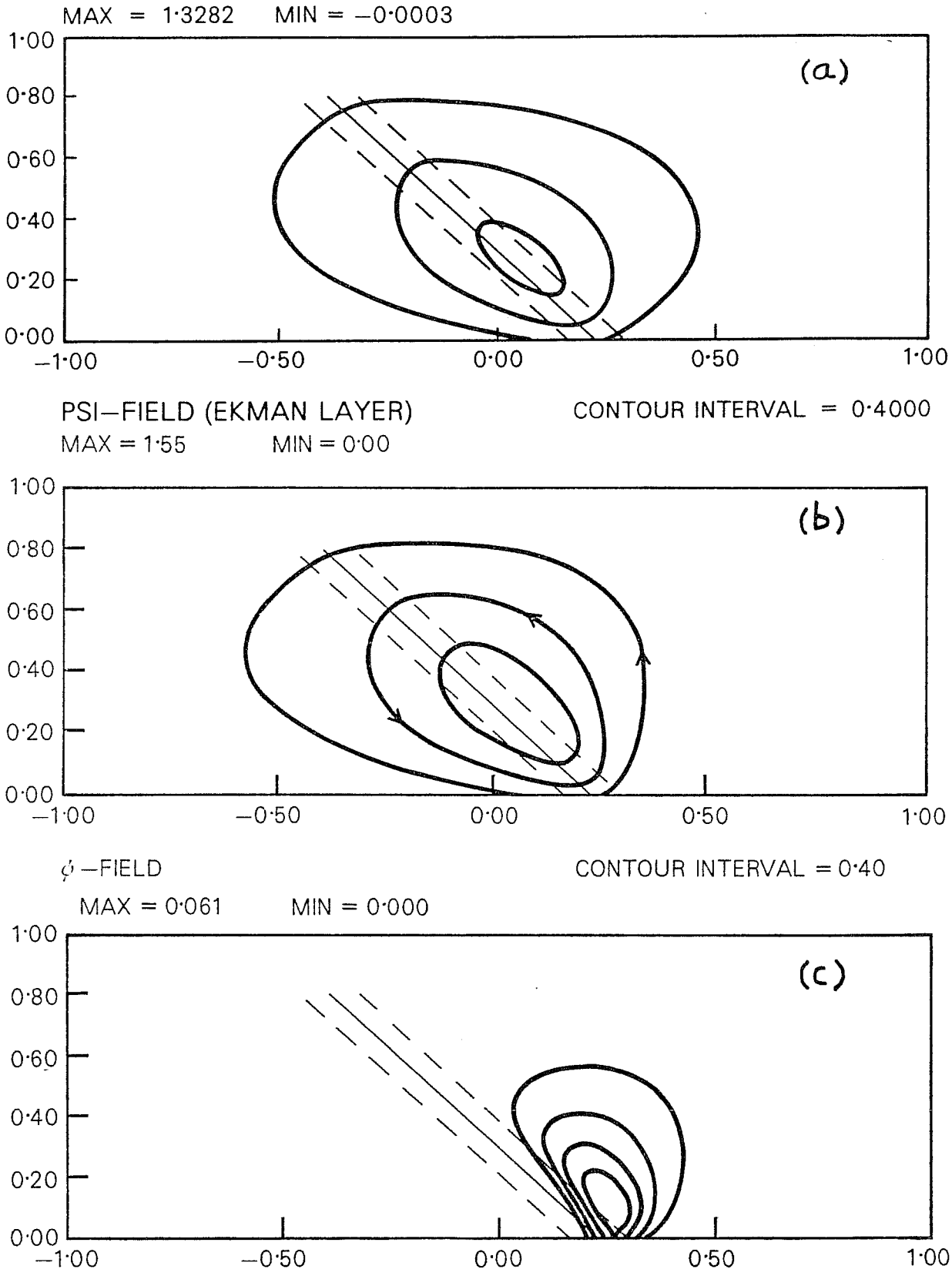

Figure 3. (a) Cross-front ageostrophic streamfunction applicable to the fields shown in Fig. 2 for no heating. (b) Streamfunction with diabatic heating proportional to the local vertical velocity ($\gamma \sim 0.9\ N^2$). Notice the more upright and intense updraught. (c) The total heating produced in case (b).

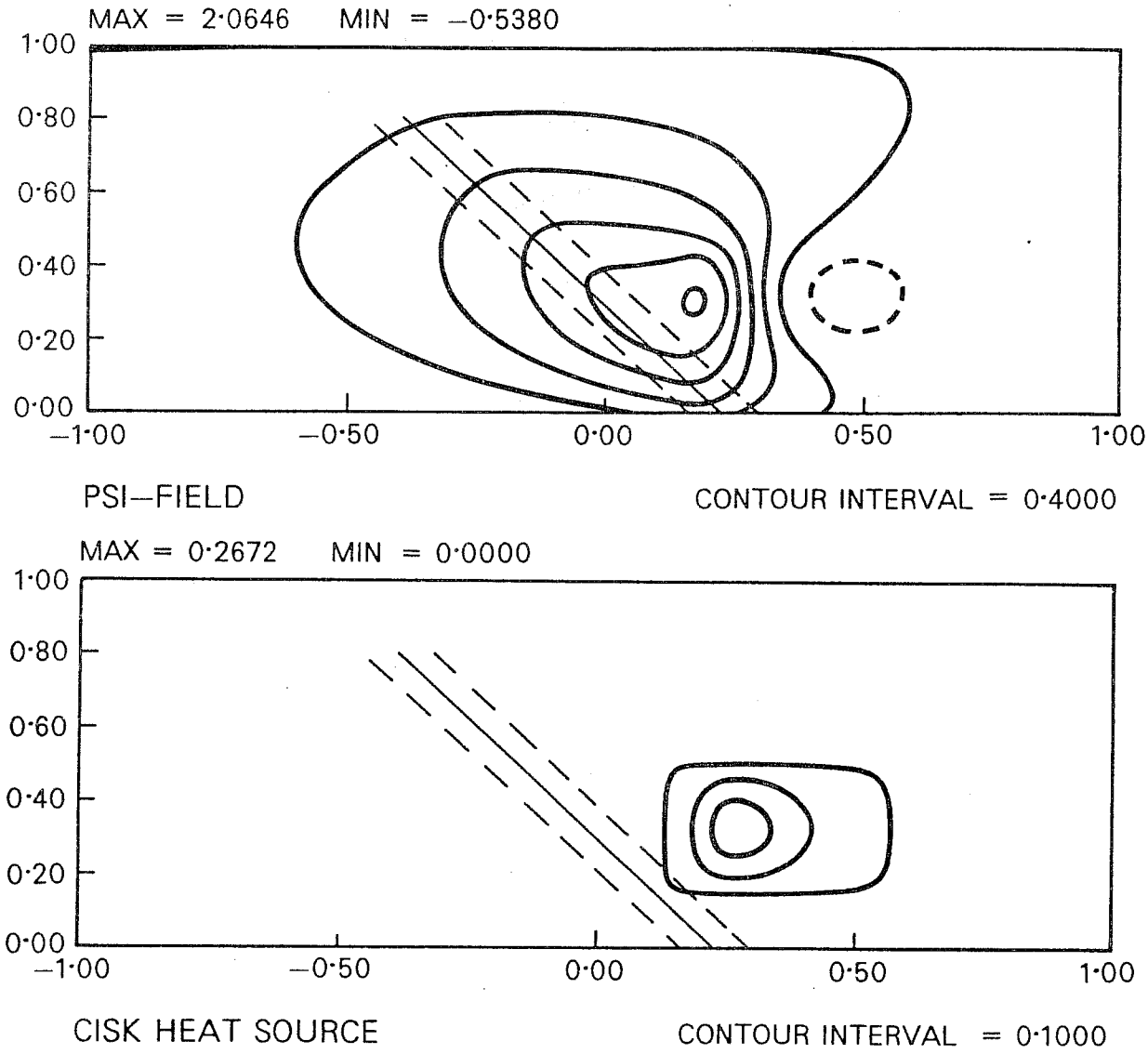

Figure 4. Cross-front streamfunction and heating for the CISK-type heating function with $b(z) \propto \sin\{\pi(z - 0.1)/0.4\}$ in the range $0.1 < z < 0.5$. [Note change in contour interval for the heating compared to Figure 3.]

Another consequence of the CISK-type scheme is that the fluid can support larger diabatic heating than the case $B = \gamma w$. In the latter scheme the ellipticity criterion limits the size of γ to a value below that which produces symmetric instability. However the evaluation of the ellipticity of the equation with CISK heating is less obvious. It appears that ellipticity is preserved if $b(z_0) < 1$ and as z_0 is the height of the top of the boundary layer where plausibly $b(z_0) = 0$ this is easily satisfied. However for $z > z_0$ the heating can be of relatively large amplitude without producing a breakdown in ellipticity and this is another consequence of the phase difference between the heating and the inherent motion.

In summary, diabatic heating in a forced baroclinic flow can produce at least two responses relying on the dependence of the source on the motion. The CISK-type scheme allows heating above a region of boundary layer convergence representing

a band of relatively vigorous convective elements. In the example shown in Figures 2-4, the heating consequently occurs in a region of more upright m-surfaces producing descent in the warm air. This is in sharp contrast to the parameterisation representing weaker sloping convection in which such descent is absent.

2.4 A rainband scale selection mechanism at fronts

The descent in the warm air produced by the CISK-type scheme provides a scale selection mechanism as it produces boundary layer divergence thus limiting the horizontal extent of the heating. It is shown in Thorpe and Nash (1983) that as the amplitude of the heating increases the scale of the band decreases. For plausible maximum heating the minimum horizontal scale is of order 100 km, typical of observations of the wide cold frontal rainband described by Matejka et al. (1980) as part of the CYCLES project. Furthermore the vertical motion produced by the heating suggests that the band will have a relatively sharp cut -off particularly on the cold air side. This is also observed in satellite pictures of active cold fronts in which the cloudiness has a sharp edge. The role of the upper level jet, which is not discussed in Thorpe and Nash (1983), is also likely to be important in this respect. Further work on the interaction of ageostrophic circulations produced by upper and lower level jets is anticipated particularly as this is likely to determine the location and scale of the convection.

2.5 Onset of mesoscale instabilities

As mentioned previously the onset of symmetric instability is related to regions with $q < 0$. It is necessary to consider whether the atmosphere is or can become unstable in this sense. The potential vorticity equation (15) shows that if the atmosphere is initially such that $q > 0$ then diabatic sources and diffusion can produce negative values of q. This may be a relatively slow process away from boundaries and regions of large condensational heating. However, in regions of near saturation the potential vorticity equation can be rewritten in terms of q_w, the wet-bulb (or equivalent) potential vorticity.

$$\frac{Dq_w}{Dt} = \frac{fg}{\theta_0}\left[\frac{g}{\theta_0}\underline{k}\cdot(\underline{\nabla}\theta\times\underline{\nabla}\theta_w) + (\underline{\zeta}\cdot\underline{\nabla})B_1\right] + DQ_w \qquad (24)$$

where B_1 is the diabatic source term due to processes <u>other</u> than latent heat release, i.e.

$$\frac{D\theta_w}{Dt} = B_1 \quad .$$

The instability criterion now becomes $q_w < 0$ and in an unsaturated atmosphere with $q_w > 0$ initially the generation of negative q_w relies on diffusion and on there being an angle between $\underline{\nabla}_h\theta$ and $\underline{\nabla}_h\theta_w$ (where suffix h indicates horizontal).

Bennetts and Hoskins (1979) suggest that this latter mechanism, which arises because moist air has a greater θ_w than dry air at the same temperature, may make q_w negative following the motion in 1-2 days. The feasibility of this process needs to be verified using observational or numerical model data.

In two-dimensional frontogenesis simulations where moisture is included there is a tendency near fronts to produce regions of low potential vorticity and suitable conditions for instability (personal communication, Caetano). The form of the instability at a front which is being forced by the synoptic scale to be frontogenetic is unknown and the subject of current research. There is some evidence in a numerical simulation (Ross and Orlanski, 1978) that the instability may rapidly decay although this was not examined in detail. However it is of interest to consider the structure of the instability in unforced regions and this forms the topic of section 3.

As an introduction to the discussion of symmetric instability it is useful to consider the representation of potential vorticity in physical space and in geostrophic momentum coordinates (X,Z). The transformation between the two coordinate systems is as follows:

$$\frac{\partial}{\partial x} = \frac{F^2}{f^2}\frac{\partial}{\partial X}$$

$$\frac{\partial}{\partial z} = \frac{S^2}{f^2}\frac{\partial}{\partial X} + \frac{\partial}{\partial Z} \qquad (25)$$

Thus it is possible to rewrite wet-bulb potential vorticity in the new coordinates:

$$q_w = \frac{fg}{\theta_0}\underline{\zeta}\cdot\underline{\nabla}\theta_w = \frac{F^2 g}{\theta_0}\frac{\partial \theta_w}{\partial Z} \qquad (26)$$

It is clear now that given inertial stability $F^2 > 0$ the symmetric instability criterion is simply that the gradient of wet-bulb potential temperature along a constant m-surface is negative. This can occur before convective instability develops as this requires the gradient of θ_w along a constant x-surface to be negative. Another way to state this is that $q_w = F^2 N_w^2 - S^4$ can be negative for $N_w^2 > 0$ so that the flow becomes symmetrically unstable before convectively unstable. A cascade of the flow to smaller scales is therefore possible in which the ageostrophic circulations ($L \sim L_R$) produce a region unstable to symmetric instability ($L \sim v/f$) which itself can become convectively unstable ($L \sim H$).

3. CONVECTIVE ORGANISATION BY MESOSCALE INSTABILITIES

3.1 Conditional symmetric instability (CSI)

Symmetric instability is a special case of three-dimensional baroclinic instability in which the zonal wavenumber is zero. This instability was first described by consideration of symmetric meridional perturbation of a circular vortex. It was pointed out by Eliassen and Kleinschmidt (1957) that the criterion for dry symmetric instability, $q < 0$ or $R < 1$, is usually not satisfied in frontal regions. However Bennetts and Hoskins (1979) suggested that if the motion were in a saturated atmospere the new criterion for instability, $q < F^2(N^2 - N_w^2)$ or $q_w < 0$, might well be satisfied at or near fronts and that this might provide an explanation for frontal rainbands. They considered ascent along a θ_w surface and dry descent along θ-surfaces. In this case rigorous linear theory is difficult due to the non-linear nature of the diabatic source term. However they provided a heuristic argument for instability and described numerical integrations of conditional symmetric instability.

It is clear that CSI is just one form of the instability and other parameterisations of the diabatic source in terms of the motion will give slightly different results. Two related forms will be discussed, in this and the next subsection, for which analytical theory is possible. The first is where both ascent and descent are along θ_w surfaces corresponding to the situation in which all the vapour condensed in the updraught is evaporated in the downdraught. In fact the structure of this instability is closely similar to that of dry SI. The second is due to Emanuel (1982) in which the diabatic term is of the CISK type described earlier in this paper and this gives rather different results involving propagating modes.

The horizontal scale of these instabilities has been a matter of some study. Emanuel(1979) showed that the scale of dry SI is a very weak function of diffusion for $L \lesssim v/f$ and therefore the scale of the instability is given typically by the horizontal projection of the θ-surfaces. Similarly, CSI, and moist SI to be described in this subsection, has a scale given by the horizontal projection of the θ_w-surface which, although slightly less than that for dry SI, is also of order 100 km.

Consider equations (1)-(5) with $k = 0$, $B = \gamma w$ and a basic geostrophic flow $V(x,z)$, i.e. $u_g = 0$, with perturbations denoted by primes which are independent of the y-coordinate. The perturbation equations are:

$$\frac{\partial u'}{\partial t} - fv' + \frac{\partial \phi'}{\partial x} = 0 \qquad (27)$$

$$\frac{\partial v'}{\partial t} + \frac{F^2}{f} u' + \frac{S^2}{f} w' = 0 \qquad (28)$$

$$\frac{\partial \phi'}{\partial z} = g \frac{\theta'}{\theta_0} \tag{29}$$

$$\frac{\partial u'}{\partial x} + \frac{\partial w'}{\partial z} = 0 \tag{30}$$

$$\frac{\partial \theta'}{\partial t} + \frac{\theta_0}{g} S^2 u' + \frac{\theta_0}{g} N_w^2 w' = 0 \tag{31}$$

A perturbation streamfunction can be introduced in the usual way and equations (27) and (29) can be combined to give:

$$\frac{\partial}{\partial t}\left(\frac{\partial^2 \psi}{\partial z^2}\right) = f \frac{\partial v'}{\partial z} - \frac{g}{\theta_0} \frac{\partial \theta'}{\partial x} \quad . \tag{32}$$

This shows that the instability grows as there is thermal wind imbalance of the eddy. Substituting into the right-hand-side of equation (32) from equations (27) and (31) gives:

$$-\frac{\partial^2}{\partial t^2}\left(\frac{\partial^2 \psi}{\partial z^2}\right) = N_w^2 \frac{\partial^2 \psi}{\partial x^2} - 2S^2 \frac{\partial^2 \psi}{\partial x \partial z} + F^2 \frac{\partial^2 \psi}{\partial z^2} \tag{33}$$

This equation with appropriate boundary conditions defines the dispersion relation and structure of the instability. It is interesting to compare this equation with equation (21) which describes the ageostrophic circulation in a forced flow. The forcing term, $-2Q$, is replaced in this case by the time development term. This is consistent with there being growth if equation (33) is hyperbolic, i.e. $q_w < 0$.

For eddies between rigid boundaries at $z = z_0$ and $z = z_1$, the solution for the vertical velocity ($w' = -\partial\psi/\partial x$) is

$$w' = \text{Real}\left[A \sin\{\nu(z - z_0)\} \exp\{i(kx + \alpha z) + \sigma t\}\right]$$

where $\nu = n\pi/(z_1 - z_0)$

$$\alpha = kS^2/(\sigma^2 + F^2)$$

$$\sigma^2 + F^2 = \frac{N_w^2 k^2}{2\nu^2}\left[\sqrt{1 + \frac{4S^4 \nu^2}{N_w^4 k^2}} - 1\right] \quad . \tag{34}$$

In the limit of k/ν large these complicated expressions reduce to:

$$\sigma^2 N_w^2 \cong S^4 - F^2 N_w^2 = -q_w$$

and $$\frac{\alpha}{k} \cong \frac{w}{S^2} \quad .$$

These results are quantitative verification of those quoted in the earlier discussion about the growth and scale of the instability. Realistic values might be $N^2 \sim 10^{-4}\ s^{-2}$, $N_w^2 \sim 2 \times 10^{-5}\ s^{-2}$, $F^2 \sim 10^{-9}\ s^{-2}$, $S^2 \sim 2 \times 10^{-7}\ s^{-2}$, giving:

$$q = +6 \times 10^{-14}\ s^{-4} \quad , \quad q_w = -2 \times 10^{-14}\ s^{-4}$$

and $\sigma^{-1} \sim 8$ hours. $\alpha/k \sim 100$ (or $L \sim 200$ km for $H \sim 2$ km).

Although these values are realistic, there is likely to be a large range of such values and observational data need to be carefully analysed to verify the applicability of the theory to frontal rainbands (see Bennetts and Sharp, 1982).

For parameterization purposes the important aspects of the theory are the transports of heat and momentum produced by the instability. These will be discussed in subsection 3.4. It is of interest however to examine the structure of the instability. In Figure 5 (overleaf) results from a simulation of CSI are reproduced (figure kindly provided by C.A. Nash, U.K. Meteorological Office). It is apparent in these simulations that the non-linear stage of development tends to produce regions, particularly near the upper boundary of the motion, in which convective instability ($\partial\theta w/\partial z < 0$) is likely. This evidence of the cascade of scales discussed earlier is of great interest but requires a more detailed numerical model to be described in adequate detail. [It should be noted that the structure of CSI can be deduced with a full nonhydrostatic equation set but the conclusions are very similar to those just described.]

3.2 Symmetric CISK

An alternative way to parameterise condensation heating using CISK has been developed by Emanuel (1982). The diabatic term related to that of equation (23) has been included in the symmetric perturbation equations. As described previously the CISK hypothesis requires the notion of a scale separation between individual convective elements and an ensemble containing a statistically steady distribution of such elements. It is therefore very different from CSI where heating following the motion of a parcel is described. However the CISK parameterisation may therefore be more applicable for inclusion in larger-scale models.

As analytical solutions were sought in this case the complicated mathematical form of equation (23) was reduced by admitting the existence of 'negative' clouds producing cooling in regions of low-level divergence. This unphysical aspect is typical of other applications of the CISK parameterisation, i.e. $B = \frac{\theta_0}{g} N^2 b(z) w_{z_0}$.

In the same way as for CSI the streamfunction equation for the eddy can be derived to be:

$$\frac{\partial^2}{\partial t^2}\left(\frac{\partial^2\psi}{\partial z^2}\right) + N^2\frac{\partial^2\psi}{\partial x^2} - 2S^2\frac{\partial^2\psi}{\partial x\partial z} + F^2\frac{\partial^2\psi}{\partial z^2} = N^2 b(z)\left.\frac{\partial^2\psi}{\partial x^2}\right|_{z_0} \qquad (35)$$

Emanuel (1982) solves equation (35) in a semi-infinite atmosphere with a radiation condition in an upper layer representing the stratosphere. The resulting dispersion relation is complicated, but for realistic parameter values there appear to be two modes. Both modes propagate towards the warm air and correspond to short- and long-wave peaks in the growth rate curves, with e-folding times of 31 hr and 24 hr and wavelengths of 380 km and 1050 km respectively. The speed of propagation is typically of order 10 m s^{-1}.

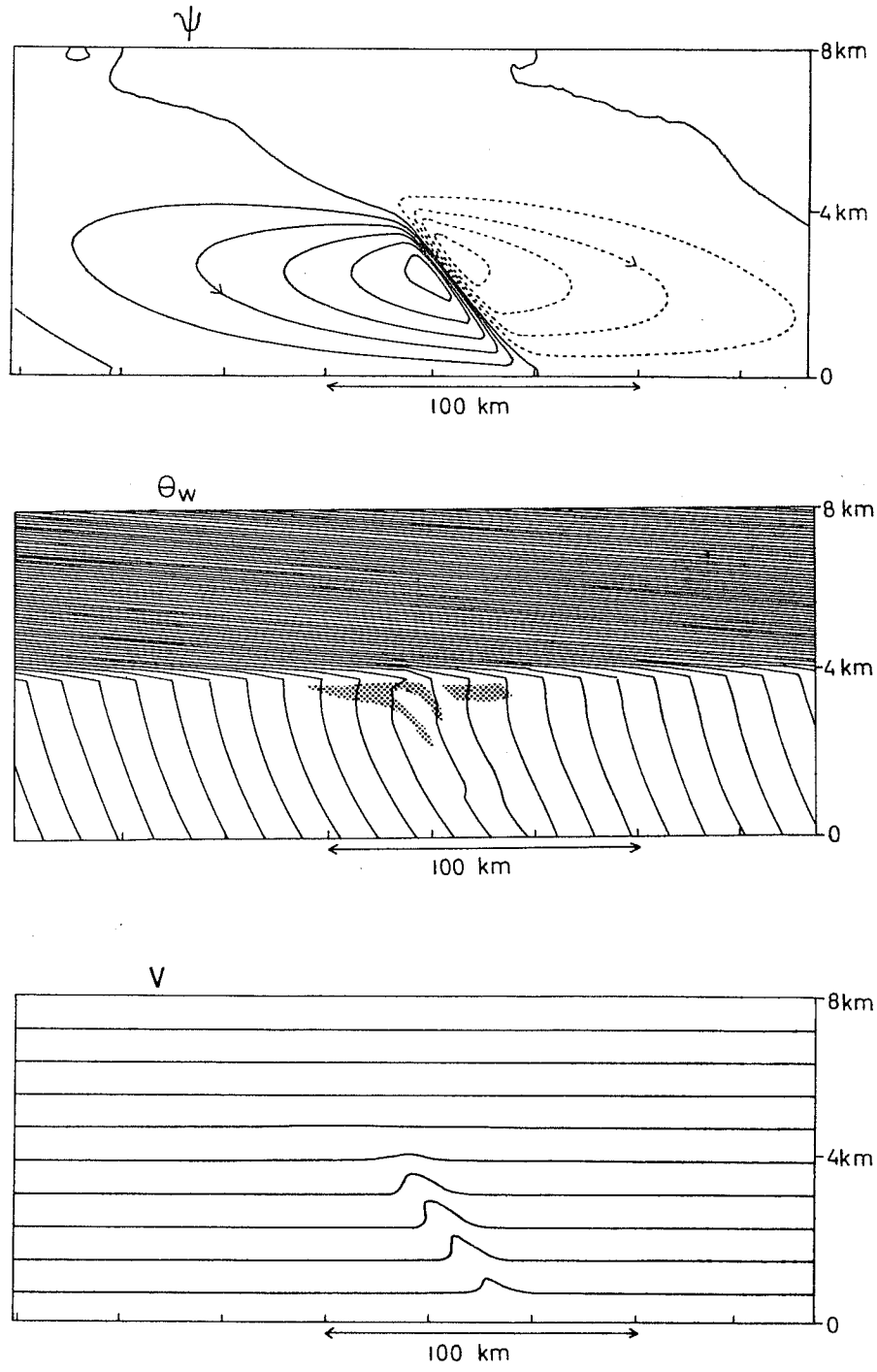

Fig. 5 Results are shown from a non-linear simulation of CSI (produced by C.A. Nash) in a periodic domain with an upper stable layer. The fields are given for a time equivalent to approximately five times the linear e-folding period. The streamfunction shows that the slope of the updraught, whilst being less than that of the θ_w-surfaces, is greater than that of the downdraughts. Regions of descent have lesser slopes than those of the m-surfaces. Also it is apparent that the right-hand cell is the least intense. The θ_w-field demonstrates the tendency to produce convectively unstable regions ($\partial\theta_w/\partial z < 0$) as shown by the dotted areas. The zonal velocity distribution is consistent with conservation of m following the motion.

These results suggest the structure of symmetric CISK to be plausibly similar to the warm sector rainbands described by Matejka et al. (1980).

Of more general interest is this demonstration of CISK in a baroclinic flow. It has been shown that CISK-modes in a barotropic flow between rigid boundaries, such as the application to tropical cyclones (Charney and Eliassen, 1964), are most unstable for $k \to \infty$ or very short waves. This is an unsatisfactory feature as it appears to contradict the original scale separation hypothesis. However in a baroclinic flow there is a finite (mesoscale) horizontal scale to the fastest growing mode and this is because the heating, which is vertically orientated, is out of phase with the motion which tends to be orientated along m or θ surfaces. This phase difference is also responsible for the existence of growing propagating modes (Bolton 1980). This feature also led to the distinctive response to CISK-type heating described in section 2.3. In a sense a CISK parameterisation is more consistently applicable to a baroclinic flow than to the barotropic flow for which it was first conceived.

3.3 Wave-mean flow interactions

As our current interest is in describing the role of the mesoscale in large-scale models, it is important to understand how these instabilities interact with the large-scale (mean) flow. In previous sections it has been shown that the large-scale flow can produce local regions in which the criterion for the onset of symmetric instability is satisfied, i.e. $q_w < 0$. However as the instability itself is two-dimensional the eddy flow conserves q_w in the absence of radiation or friction. It is therefore pertinent to ask if a steady-state or even a decay phase is possible for CSI. Various mechanisms are possible to limit the growth of CSI and these include: radiation, diffusion of heat and momentum, and breakdown to non-symmetric or convective motion. Although Walton (1975) has shown that a finite amplitude viscous steady state is possible the numerical simulations indicate that a breakdown to upright convective ($\partial\theta_w/\partial z < 0$) motion is more likely. In that case evaporative cooling, dry subsidence, and mixing are likely to be sources of q_w.

The equation for the rate of change of eddy kinetic energy can be shown to be:

$$\frac{1}{2}\frac{\partial}{\partial t}\int_{z_0}^{z_1}(\overline{u'^2} + \overline{v'^2})dz = -\int_{z_0}^{z_1}\left(\overline{u'v'}\ \frac{\partial v}{\partial x} + \overline{v'w'}\ \frac{\partial v}{\partial z} - \frac{g}{\theta_0}\overline{w'\theta'}\right)dz \qquad (36)$$

where the overbar is an average over one horizontal wavelength.

Using the solution quoted in section (3.1), the flux terms can be evaluated as:

$$\overline{u'v'} = \frac{-|A|^2}{2\sigma f}\left\{\frac{F^2\nu^2}{k^2}\cos^2\left(\nu(z-z_0)\right) - \frac{S^4\sigma^2}{(\sigma^2+F^2)^2}\sin^2\left(\nu(z-z_0)\right)\right\}e^{2\sigma t}$$

$$\overline{v'w'} = \frac{-|A|^2\,\sigma\,S^2}{2f(\sigma^2+F^2)}\sin^2\left(\nu(z-z_0)\right)e^{2\sigma t}$$

$$\overline{w'\theta'} = \frac{\theta_0|A|^2\left(|q_w| - N_w^2\sigma^2\right)}{2g\,\sigma\,f(\sigma^2+F^2)}\sin^2\left(\nu(z-z_0)\right)e^{2\sigma t} \quad . \tag{37}$$

Thus the second term on the right-hand side of equation (37) is positive, for $\partial v/\partial z > 0$, indicating that the eddy extracts kinetic energy from mean vertical shear. The third term is positive but small as $\sigma^2 \sim |q_w|/N_w^2$. The first term is more complicated but for $\partial v/\partial x > 0$ it too can be shown to be positive.

The momentum and heat transport equations can be deduced by making an expansion of the eddy fields using a small parameter ε which might be $(V_z H/f)/L_R \sim 0.1$:

$$v = V + \varepsilon v' + \varepsilon^2 v_2 + \ldots$$

$$u = \varepsilon u' + \varepsilon^2 u_2 + \ldots$$

$$w = \varepsilon w' + \varepsilon^2 w_2 + \ldots$$

$$\theta = \theta_0 + \varepsilon\theta' + \varepsilon^2\theta_2 + \ldots \quad \text{etc.}$$

Taking a horizontal average over one wavelength allows the mean flow to be written, for example, as:

$$\bar{v} = V + \varepsilon^2\bar{v}_2 + \ldots$$

$$\bar{u} = \varepsilon^2\bar{u}_2 + \ldots \quad \text{etc.}$$

It can be seen that the x-averaged second order term, which is in fact non-zero, is the change in the mean flow caused by the eddy. These changes satisfy the equations:

$$\left.\begin{aligned}
&\frac{\partial\bar{u}_2}{\partial t} - f\bar{v}_2 = -\frac{\partial}{\partial z}\left(\overline{u'w'}\right)\\
&\frac{\partial\bar{v}_2}{\partial t} + \frac{F^2}{f}\bar{u}_2 = -\frac{\partial}{\partial z}\left(\overline{w'v'}\right)\\
&\bar{w}_2 = 0\\
&\frac{\partial\bar{\theta}_2}{\partial t} + \frac{\theta_0}{g}S^2\bar{u}_2 = -\frac{\partial}{\partial z}\left(\overline{w'\theta'}\right)
\end{aligned}\right\} \tag{38}$$

Solutions to these equations are:

$$\left.\begin{aligned}
&\bar{u}_2 = \frac{3|A|^2\,S^2\,\nu}{2(\sigma^2+F^2)(F^2+4\sigma^2)}\,G(z,t)\\
&\bar{v}_2 = \frac{|A|^2\,S^2\,\nu(2\sigma^2-F^2)}{2f(\sigma^2+F^2)(F^2+4\sigma^2)}\,G(z,t)\\
&\bar{\theta}_2 = \frac{-|A|^2\,\nu\,\theta_0}{4g\sigma(\sigma^2+F^2)}\left[\frac{|q_w| - N_w^2\,\sigma^2}{f} + \frac{S^4}{(F^2+4\sigma^2)}\right]G(z,t)
\end{aligned}\right\} \tag{39}$$

where $G(z,t) = \sin[2\nu(z - z_0)]\exp(2\sigma t)$.

These are similar to the solutions derived by Stone (1972) in the case $F^2 = f^2$. It can be shown that $\bar{u}_2 > 0$, $\bar{v}_2 > 0$, and $\bar{\theta}_2 < 0$ in the lower half of the domain and that they have the opposite sign in the upper half. This indicates for example that the mean shear is reduced by the eddy.

Whilst these solutions represent the changes to the mean flow local to the eddy they do not represent the quasi (or semi) geostrophic adjustment of a baroclinic flow to a localised region of instability. The local corrections to the mean flow represented by the second order eddy terms are likely to be insignificant to the larger scale ($\sim L_R$) ageostrophic circulations produced as the flow responds to the presence of the eddy forcing. To calculate this adjustment, which incidentally would form the basis of a parameterization scheme for inclusion in a large-scale model, the equations in section 2.1 need to be rewritten with source terms representing the fluxes of heat and momentum produced by a localized region of instability. In this way the role of symmetric instability at fronts can be assessed. This problem is one of current development and the appropriate equations seem to be:

$$\left.\begin{aligned} \frac{D\bar{v}}{Dt} + f\bar{u}_a &= -\frac{\partial}{\partial z}(\overline{v'w'}) \\ \frac{D\bar{\theta}}{Dt} &= B - \frac{\partial}{\partial z}(\overline{w'\theta'}) \end{aligned}\right\} \qquad (40)$$

with an extra forcing term on the right-hand side of the Sawyer-Eliassen equation given by:

$$-f\frac{\partial^2}{\partial z^2}(\overline{v'w'}) + \frac{g}{\theta_0}\frac{\partial^2}{\partial x \partial z}(\overline{w'\theta'})$$

where the second term is likely to be much smaller than the first.

The overbar on the terms on the left-hand side of equation (40) indicate the inclusion of the small correction to the flow local to the region of parameterized instability. Solutions to these equations are being investigated in an attempt to test these ideas as a viable parameterization scheme.

4. PARAMETERISATION OF CONVECTION AT FRONTS

4.1 Synoptic-scale diagnosis of frontogenesis

Following the work of Hoskins and Pedder (1980) and Hoskins, Draghici and Davies (1978), it is possible in a simple way to diagnose from the synoptic scale data regions of active frontogenesis. From such a diagnosis the location of convection at fronts could be deduced so that convective parameterisation schemes can be used there. The basis of the synoptic scale diagnosis is the quasi-geostrophic omega equation which can be deduced by taking equations (8) → (12) but using the

geostrophic wind for the advection terms in the substantial derivative. Performing the same manipulations described in section 2.1 gives the equation:

$$N^2 \nabla_h^2 w + f^2 \frac{\partial^2 w}{\partial z^2} = \frac{2g}{\theta_0} \underline{\nabla} \cdot \underline{Q} \quad , \tag{41}$$

where w is the vertical velocity and $\underline{Q}$ is the Q-vector given by

$$\underline{Q} = \left(- \frac{\partial \underline{v}_g}{\partial x} \cdot \underline{\nabla}\theta \ , \ - \frac{\partial \underline{v}_g}{\partial y} \cdot \underline{\nabla}\theta \right) \quad .$$

Thus regions of convergence in $\underline{Q}$ correspond to ascent and regions of divergence correspond to descent. At a front it is easy to see that this pattern of vertical motion is consistent with a thermally direct circulation about the front. Examples of the practical application of this diagnosis can be found in Hoskins and Pedder (1980) and Buzzi and Speranza (1983), the latter case being one of cyclogenesis over the Alps. As described in Hoskins and Pedder (1980) the routine analysis of Q-vectors is more informative than, say, the vertical velocity, as they convey more information. In particular analyses of Q-vector plots indicate ageostrophic motion, ageostrophic vorticity, and tendency for frontogenesis or frontolysis. A superposition of the Q-vector analysis and the moisture analysis would give a good indication of those regions where the implied ascent might be enhanced by latent heat release.

4.2 Sloping and upright convection

The location of regions, fronts, where release of latent heat is likely can be ascertained as just described. The nature of the convection which then occurs has been the subject of the earlier part of this paper. A simple criterion is that if $q_w < 0$, or equivalently $\partial\theta_w/\partial Z < 0$, then moist symmetric instability and associated transports of heat and momentum will occur.

The amount of potential energy available for such slantwise or sloping convection can be estimated following Emanuel (1983). The total slantwise convective available potential energy (SCAPE) is the sum of the CAPE (positive area on a tephigram) and a contribution from centrifugal forces:

$$\text{SCAPE} = \text{CAPE} + \int_{z_0}^{z_1} \frac{f^2}{2F^2} \frac{d}{dz} \{(v - v_0)^2\} dz \quad ,$$

where F^2 has been assumed to be a function of z only, and $(v - v_0)$ is the difference between v of the parcel and that of its environment. The parcel v can be obtained as $m = v + fx$ is conserved following the motion. For F^2 a constant the expression simplifies to:

$$\text{SCAPE} = \text{CAPE} + \frac{1}{2} \frac{f^2}{F^2} (v_1 - v_0)^2 \ ,$$

where $v_1 - v_0$ is the difference in zonal velocity between the top and bottom of the layer subject to the instability. Emanuel (1983) makes the point that the second

term, representing the available kinetic energy, can be a substantial contribution even compensating for significant negative CAPE. Thus if SCAPE > 0 the moist baroclinic atmosphere is unstable to finite slantwise parcel displacements in two dimensions. This criterion is rather different from $q_w < 0$ which is only applicable to infinitesimal displacements in a saturated atmosphere. Furthermore, the atmosphere can be stableto upright convection (vertical displacements) with CAPE < 0 but unstable to slantwise convection (m-surface displacement) for SCAPE > 0.

It would seem likely that moist symmetric instability would continue until $\partial\theta_w/\partial Z = 0$ or $q_w = 0$ although, as mentioned previously, it is unclear exactly how this fluid stabilization takes place. Thus a parameterisation for the heat transport by symmetric instability involves 'mixing' θ_w along constant absolute momentum surfaces. This possibility is examined further in the next section by appropriate solutions of the circulation equation.

Observations indicate that regions of active upright convection occur at fronts. The results from numerical simulations of CSI also show that convective instability can be produced as a consequence of advection in a symmetric circulation. It is apparent from the results presented in section 2.3 of the effects of diabatic heating in a forced baroclinic flow that upright convection cannot be parameterised by a heat source proportional to the local vertical velocity as would be the case in a barotropic flow. It would appear that the CISK-type of heating function is most appropriate in a baroclinic flow for the representation of upright convection. The heating should be orientated vertically as described by the relationship in equation (23).

4.3 Parameterisation of heating due to sloping convection

As stated in the last section it seems likely that a region of CSI will tend to mix θ_w along m-surfaces. Some solutions of the circulation equation will now be described including such a parameterisation. To release latent heat along m-surfaces the circulation equation in geostrophic momentum coordinates will be used, i.e. equation (16). The simplest case is for constant q, that is, a constant gradient baroclinic zone:

$$q = F^2N^2 - S^4 = F^2N^2(R - 1)/R \quad ,$$

where $R = F^2N^2/S^4$ is a Richardson number for the zone.

It is convenient to non-dimensionalize equation (16) in the following way:

$$(\bar{X},\bar{Z}) \rightarrow \left(\frac{Xf^2}{NHF}\sqrt{\frac{R}{R-1}}\,,\ \frac{Z}{H}\right)$$

$$(\bar{\psi},\bar{Q},\bar{B}) \rightarrow \left(\frac{\psi f}{H^2S^2}\,,\ \frac{Qf}{F^2S^2}\,,\ \frac{gBf}{\theta_0 S^2 HNF}\sqrt{\frac{R}{R-1}}\right)$$

Thus equation (16) becomes:

$$\bar{\psi}_{\bar{X}\bar{X}} + \bar{\psi}_{\bar{Z}\bar{Z}} = -2\bar{Q} - \bar{B}_{\bar{X}} \quad . \tag{42}$$

Solutions of equation (42) will be presented for a geostrophic forcing given by:

$$\bar{Q} = \bar{Q}_0 \sin\left(\left(\frac{\bar{X} - \bar{X}_0}{\bar{X}_1 - \bar{X}_0}\right)\pi\right) \sin\left(\left(\frac{\bar{Z} - \bar{Z}_0}{\bar{Z}_1 - \bar{Z}_0}\right)\pi\right) \quad \text{for } \bar{X}_0 < \bar{X} < \bar{X}_1 \text{ and } \bar{Z}_0 < \bar{Z} < \bar{Z}_1 \quad ,$$

with $\bar{X}_0 = -0.04$, $\bar{X}_1 = 0.04$, $\bar{Z}_0 = 0.2$, $\bar{Z}_1 = 0.3$ and $\bar{Q}_0 = 0.5$.
Various forms for the diabatic term will be used:

(a) $\bar{B} = 0$

(b) $\bar{B} = -\bar{B}_0\left(\bar{\psi}_{\bar{X}} + |\bar{\psi}_{\bar{X}}|\right)$

(c) $\bar{B} = -\bar{B}_1\left(\bar{\psi}_{\bar{X}}(\bar{Z}_0) + |\bar{\psi}_{\bar{X}}(\bar{Z}_0)|\right)b(\bar{Z})$

where $b(\bar{Z}) = \sin\left(\left(\frac{\bar{Z} - \bar{Z}_0}{1 - \bar{Z}_0}\right)\pi\right)$, with $\bar{Z}_0 = 0.1$, for $\bar{Z}_0 < \bar{Z} < 1$.

Thus (a) represents no heating, (b) heating proportional to the local vertical velocity, and (c) heating of the CISK type constant along $\bar{X}$ (equivalent to m) surfaces). In figure 6 solutions are shown in which the heating amplitudes are as quoted (note the streamfunction is shown in physical coordinates and not geostrophic momentum coordinates).

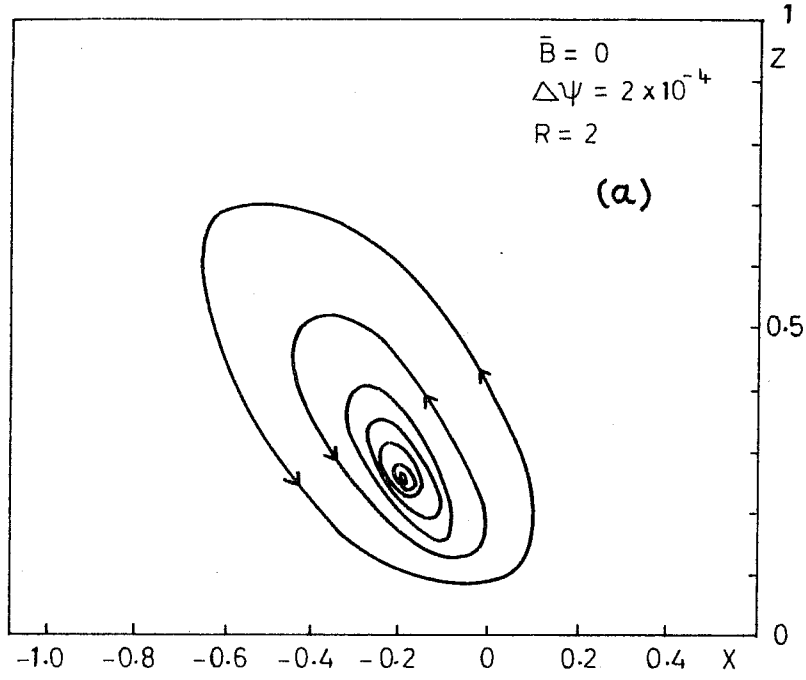

Figure 6(a)
[Caption opposite]

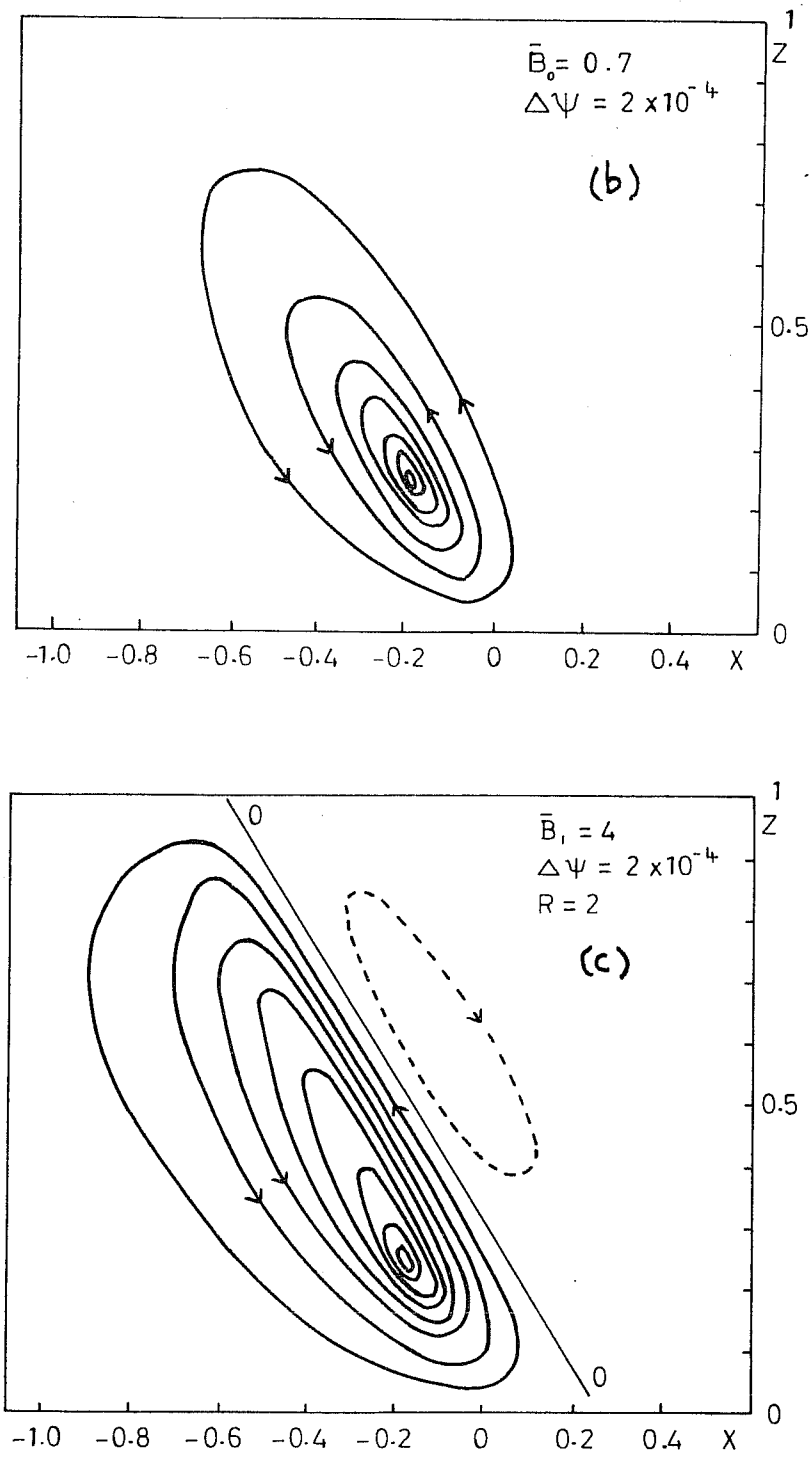

Figure 6. Cross-front streamfunction for the case of a uniform baroclinic zone with a localised Q-forcing: (a) with no heating, (b) with heating proportional to the local vertical velocity, and (c) with CISK-type heating representing mixing of θ_w along m (or X surfaces).

The CISK-type formulation is most likely to represent heating due to mixing of θ_w along m-surfaces. This is because the amount of heating in this situation is likely to be related to the moisture convergence at low levels and to the value of SCAPE. The amplitude $\bar{B}_1$ can be thought to be proportional to the SCAPE. The alternative parameterisation in which $\bar{B}$ is proportional to the local w is less realistic as the (unresolved) CSI will produce a heating distribution, along m surfaces, related to its vertical velocity and not that of the forced circulation. This distribution, given by $b(Z)$, has been taken to be a simple sinusoid, a form which is consistent with the numerical simulations of CSI.

It is apparent that, similar to the results in section 2.3, there are different responses to the two heating functions. The more realistic CISK formulation produces an intensification of the updraught and a region of descent in the warmer air. Although at the time of writing no quantitative calculations of the frontogenesis have been made it appears that the presence of sloping convection has increased the frontogenetic tendency of the ageostrophic circulation. Clearly these results could be extended to include evaporatively cooled downdraughts produced by precipitation from the rainband. It would seem plausible to suggest that the role of the downdraughts would be to produce frontolysis near the surface although this needs to be shown by further modelling.

The practical application of this parameterisation of sloping convection in large-scale models is not entirely straightforward. As shown the scheme is most naturally formulated in geostrophic momentum coordinates. However these results suggest that parametrisation of slant-wise convection may be of considerable importance in adequate representation of mesoscale processes.

4.4 Parameterisation of momentum transports

In section 3.3 the problem of momentum transport by moist symmetric instability was discussed. Although the local wave-mean flow interactions have been calculated, it is not clear how the atmosphere on the scale larger than the region of instability adjusts to the fluxes of momentum produced by the eddy. However it is likely that the momentum fluxes will represent an important forcing of the large-scale flow.

The flux source terms in equation (40) are given from linear theory by the expressions in equation (37). The transport of momentum is downgradient and in the limit of large k/ν the flux becomes:

$$\overline{v'w'} = -\sqrt{1 - \frac{F^2 N_w^2}{S^4}}\,\frac{N_w}{2f}\,|A|^2 \sin^2\left(\nu(z - z_0)\right) \exp(2\sigma t)$$

This expression is not of the eddy viscosity type in which the flux is proportional to the mean gradient (S^2), although it is apparent that as S^2 increases so does the momentum flux.

By way of contrast the momentum fluxes associated with some types of upright convection are relatively well understood. Using the concept of steady convective overturning, rather than linear theories which have proved rather unsatisfactory for deep convection, appropriate momentum and heat fluxes have been deduced (see article by Moncrieff and Miller). However, as yet these appear applicable only to fluxes normal to the convective band or squall line. In the present nomenclature this corresponds to specifying $\overline{u'w'}$. Of particular interest in the frontal case is the flux of momentum in the zonal direction which is parallel to the convective line. As yet there has been little work done on simulating deep convective bands in the presence of strong shears parallel to the line. This would appear to be a fruitful line of research as observations of line convection, for example, at fronts indicate this to be a common feature. It is likely that the momentum transports associated with such a system are of a distinctly different form to those calculated for systems in which the along-line wind shear is small.

5. DISCUSSION

This paper has attempted to review current ideas on the structure of convection in baroclinic environments with particular reference to fronts. It is apparent that dynamical theories of both slantwise and upright convection are emerging which give a new perspective on the nature of the mesoscale. Consequently it is appropriate to regard the mesoscale as a fundamental link between the synoptic scale and the cloud scale in frontal systems.

There are several explanations postulated for the mesoscale organization of convection which have not been described in this paper. These include ducted internal gravity waves (Lindzen and Tung, 1976), gravity waves generated during the frontal scale collapse (Ley and Peltier, 1978), and Kelvin-Helmholtz instabilities. Whilst important in producing localized regions of flow perturbation they do not, in general, consider the structure of the convection itself. The theories examined in this paper all describe how latent heat due to condensation is released in a baroclinic flow. Furthermore moist symmetric instability is capable of defining a mesoscale structure in a baroclinic environment which more general gravity wave descriptions do not take into specific account.

In particular, as suggested in the title of the paper, there is a distinctive role played by the CISK-type parameterisations of diabatic heating in baroclinic flows. For upright convection this description allows the convective band, probably made up of many individual elements, to have an upright structure despite the inherent shallow motion typical of ageostrophic circulations at fronts which slopes along constant absolute momentum surfaces. Furthermore the diabatic heating involved in such bands produces descent outside the band which acts as a scale selection

mechanism. Fot slantwise convection the CISK-type parameterisation can also be used if the heating is released along m-surfaces. This method is most immediately applicable to models using the semigeostrophic equations and the geostrophic momentum coordinates. In this latter application of CISK the heating represents the mixing of θ_w along m-surfaces typical of the effect of moist symmetric instability.

There are many problems still left unanswered. How does CSI evolve in the nonlinear phase and in particular how does the instability eventually decay by stabilization of its environment? What is the structure of the instability in a region forced by the synoptic scale to be frontogenetic? What are the momentum transports produced by a localised region of instability, and how does upright convection develop in a frontal environment? Answers to these questions will increase the basic understanding of moist processes near fronts and also allow specification of parameterisation schemes suitable for large-scale models.

REFERENCES

Bennetts, D.A. and Hoskins, B.J., 1979. Conditional symmetric instability - a possible explanation for frontal rainbands. Quart J.R. Met. Soc., 105, 945-962.

Bennetts, D.A. and Sharp, J.C., 1982. The relevance of conditional symmetric instability to the prediction of mesoscale frontal rainbands. Ibid., 108, 595-602.

Bolton, D., 1980. Application of the Miles theorem to forced linear perturbations. J. Atmos. Sci., 37, 1639-1642.

Buzzi, A. and Speranza, A., 1983. Cyclogenesis in the lee of the Alps. Mesoscale Meteorology - theories, observations and models, Reidel.

Charney, J.G., 1973. Planetary fluid dynamics, Dynamic Meteorology, Reidel (ed. P. Morel).

Charney, J.G. and Eliassen, A., 1964. On the growth of the hurricane depression. J. Atmos. Sci., 21, 68-75.

Eliassen, A., 1952. Slow thermally or frictionally controlled meridional circulation in a circular vortex. Astrophys. Norv., 5, 19-60.

Eliassen, A., 1962. On the vertical circulation in frontal zones. Geofys. Publikasjoner, 24, (No. 4), 147-160.

Eliassen, A. and Kleinschmidt, E., 1957. Dynamic meteorology. Handbuch der Physik, 48, Springer Verlag.

Emanuel, K.A., 1979. Inertial instability and mesoscale convective systems. Part I: Linear theory of inertial instability in rotating viscous fluids. J. Atmos. Sci., 36, 2425-2449.

Emanuel, K.A., 1982. Inertial instability and mesoscale convective systems. Part II: Symmetric CISK in a baroclinic flow. Ibid., 39, 1080-1096.

Emanuel, K.A., 1983. On the dynamical definition(s) of "mesoscale". Mesoscale meteorology - theories, observations and models, Reidel.

Emanuel, K.A., 1983. On assessing local conditional symmetric instability from atmospheric soundings (accepted by Mon. Wea. Rev.)

Gill, A.E., 1982. Atmosphere-ocean Dynamics, Academic Press.

Hoskins, B.J. and Bretherton, F.P., 1972. Atmospheric frontogenesis models: mathematical formulation and solution. J. Atmos. Sci., 29, 11-37.

Hoskins, B.J., Draghici, I., and Davies, H.C., 1978. A new look at the ω-equation. Quart. J. R. Met. Soc., 104, 31-38.

Hoskins, B.J. and Heckley, W.A., 1981. Cold and warm fronts in baroclinic waves. Ibid., 107, 79-90.

Hoskins, B.J. and Pedder, M.A., 1980. The diagnosis of middle latitude synoptic development. Ibid., 106, 707-719.

Ley, B.E. and Peltier, W.R., 1978. Wave generation and frontal collapse. J. Atmos. Sci., 35, 3-17.

Lindzen , R.S. and Tung, K.-K., 1976. Banded convective activity and ducted gravity waves. Mon. Wea. Rev., 104, 1602-1617.

Matejka, T.J., Houze, R.A. and Hobbs, P.V., 1980. Microphysics and dynamics of clouds associated with mesoscale rainbands in extratropical cyclones. Quart. J. R. Met. Soc., 106, 29-56.

Moncrieff, M.W. and Miller, M.J., 1976. The dynamics and simulation of tropical cumulonimbus and squall lines. Ibid., 102, 373-394.

Ooyama, K., 1982. On basic problems in theory and modelling of the tropical cyclone. Topics in Atmospheric and Oceanographic Sciences (Intense atmospheric vortices), Springer-Verlag.

Orlanski, I., 1975. A rational subdivision of scales for atmospheric processes. Bull. Am. Met. Soc., 56, 527-529

Ross, B.B. and Orlanski, I., 1978. The circulation associated with a cold front. Part II. Moist case. J. Atmos. Sci., 35, 445-465.

Sawyer, J.S., 1956. The vertical circulation at meteorological fronts and its relation to frontogenesis. Proc. Roy. Soc. A. 234, 346-362.

Stone, P.H., 1972. On non-geostrophic baroclinic stability. Part III. The momentum and heat transports. J. Atmos. Sci., 29, 419-426

Thorpe, A.J., 1983. Note on convective parameterisations in a quasi-geostrophic diagnostic model of fronts. (Accepted for publication in J. Atmos. Sci.)

Thorpe, A.J., Miller, M.J. and Moncrieff, M.W., 1982. Two dimensional convection in non-constant shear: a model of mid-latitude squall lines. Quart. J. R. Met. Soc., 108, 739-762.

Thorpe, A.J. and Nash, C.A., 1983. Convective and boundary layer parameterisations in a diagnostic of atmospheric fronts. (Submitted to Quart.J.R.Met. Soc.)

Walton, I.C., 1975. The viscous nonlinear symmetric baroclinic instability of a zonal shear flow. J. Fluid Mech., 68, 757-768.